Reduction of a conductance-based model for individual neurons

Jingxin Ye and Marvin Thielk

December 15, 2012

Abstract

We investigated schemes to systematically reduce the number of of different of differential equations required for biophysically realistic neuron model. The original scheme is invented by Thomas Kepler in 1992, and it is used in many neuronal models, such as Hodgkin-Huxley, A-current model and a stomatogastric neuron model.

The general idea of this scheme is to inverse all the gating variable equations to get corresponding equivalent potential. We base the reduction on the fact that some of those potentials have similar wave forms with the membrane potential or the other equivalent potentials. We use singular perturbation theory and principal component analysis to analyze the reduction. We successfully reduce the phase-dimensionality of a realistic HVC neuron model from 12 to 3. The membrane potential and equivalent potentials have identical behavior in both the reference and reduced model and it holds for arbitrary injected current under certain parameters.

1 Introduction

Neural networks are composed of individual neurons interacting via synapses. For better understanding and simpler analysis of network models, models of each neuron should be as simple as possible while retaining essential biological features. The most remarkable biological individual neuron model is put forward by Hodgkin and Huxley [1]. The Hodgkin-Huxley model is a four-variable model describing the generation of action potentials in the squid giant axon based the properties of the neuron's ionic channels. Analysis of H-H model shows that it contains two kinds of variables: excitation variables and recovery variables. Under this idea, Fitzhugh and Nagumo proposed a two-dimensional reduced model with the membrane potential and slow recovery variables. Early computer simulation by Krinskii and Kokoz [2] has shown that there is linear relationship between the gating variables $n(t)$ and $h(t)$. Finding numerical relationships between several variables is an essential process in dimension reduction.

Later, Kepler et al. [3] introduced a more systematic reduction method called "equivalent potentials" to discover those relationships among gating variables. They reduced the H-H model to a two-dimensional system by using the instantaneous m approximation and combining the variables h and n, which have a similar time scale. This

method has been wildly applied: Kepler et al. [3] reduced a modification of H-H to which the A current has been added. The six-dimensional model was reduced to a three-dimensional one by introducing three time scales: the fast one of V and m, the slower one of h, n and a_A, and the slowest one of b_A. Thereafter, this method has been extended to simplify other rich, physiologically realistic models. A stomagtogastric ganglion LP neuron containing 13 dynamical variables was simplified to seven-dimensional one [4]; And the eight variables for the giant neuron localized in the espohageal ganglia of the marine pulmonate mollusk Onchidium verruculatum has been reduced to four-and-three-dimensional systems by regrouping variables with similar time scales [5].

Meliza et al. [6] created a detailed conductance-based model for the neurons from zebra finch HVC. This 12-dimensional model is described in Section 2. We have produced a three-dimensional reduced model that yields similar dynamical behavior. We describe the reduction we made to the 12-dimensional model in Section 3. Our attempt to analyze the potential reduction using principal component analysis is described in Section 4. The two models are compared and the results are summarized in Section 5 and 6.

2 Reference Model for HVc neuron

2.1 Structure of Model

The conductance-based mathematical model of HVc neuron is the starting point of this project. It is a single compartment isopotential model with a passive leak conductance and eight active, voltage-gated conductances. The selection of sodium, potassium, calcium, and nonselective cation channels that have been found in a broad range of neurons, which can be regarded as an extension of H-H model with additional current taken into account. In the following, we give a brief description of this model, which we refer to as the reference model.

The change in the electrical potential of the model neuron is casued by the accumulation of currents that flow through channels located within the membrane and an external current injected through an electrode. The cell is assumed to be isopotential with its membrane potential V, satisfying the equation:

$$C_m \frac{dV}{dt} = \frac{I_{ext}}{I_{\mathrm{SA}}} + I_{\mathrm{Na_T}} + I_{\mathrm{Na_P}} + I_{\mathrm{K_{A1}}} + I_{\mathrm{K_{A2}}} + I_{\mathrm{K_3}} + I_{\mathrm{h}} + I_{\mathrm{Ca_L}} + I_{\mathrm{Ca_T}} + I_{\mathrm{Leak}}$$

where C_m is the membrane capacitance and each of the voltage-gated currents I_j's depends on ion ow through channels whose permeability is controlled by activation (x) and inactivation (y) gating variables:

$$I_j = g_j \, x^{N_1} \, y^{N_2} \, (E_{reversal} - V)$$

where g_j is maximum conductance and N_1 and N_2 are integers. The voltage-gated currents we include are:

- $I_{\mathrm{Na_T}}$ is transient sodium current. This current is strongly voltage dependent and is largely responsible for generating action potentials. Its kinetics can be represented by m^3h, and m is a fast variable.
- $I_{\mathrm{Na_P}}$ is persistent sodium current, and its kinetics are represented by n.
- $I_{\mathrm{K_{A1}}}$ is non-inactivating fast potassium current. It has no significant inactivation and thus it is represented by m^4
- $I_{\mathrm{K_{A2}}}$ is inactivating potassium current whose kinetics are represented by p^4q.
- $I_{\mathrm{K_3}}$ is slow potassium current, and kinetics are represented by u.
- I_{h} is hyperpolarization-activated cation current. A mixed cation current that typically activates with hyperpolarizing steps to potentials negative to -50 to -60 mV. The kinetics of activation during a hyperpolarization, and deactivation following repolarization, are complex. Its kinetics is simply represented by z.
- $I_{\mathrm{Ca_L}}$ is the high-threshold L-type calcium current whose kinetics are determined by s^2t.
- $I_{\mathrm{Ca_T}}$ is the low-threshold T-type calcium whose kinetics are represented by r^2.
- I_{Leak} is the leak current. It is not voltage dependent in our model, and it is represented only by its constant maximal conductance g_l

The dynamics of the ion channel gating elements are given by voltage-dependent opening and closing rates. To ensure numerical stability, we use a hyperbolic tangent approximation to the Boltzmann barrier-hopping rate

$$\begin{aligned}
\frac{dx}{dt} &= \frac{x_\infty(V) - x}{\tau(V)} \\
x_\infty &= \frac{1}{2}\left[1 + \tanh\left(\frac{V - V_{1/2}}{\kappa}\right)\right] \\
\tau(V) &= \tau_0 + \tau_{\max}\left[1 - \tanh^2\left(\frac{V - V_{1/2}}{\sigma}\right)\right]
\end{aligned}$$

where $V_{1/2,j}$ is the half-activation voltage, κ_j is the slope of the activation function between the closed and open state, τ_0 is the minimum relaxation time, $\tau_0 + \tau_{\max}$ is the peak relaxation time, and σ_j is the width of the relaxation time function. Equations for the inactivation variables (y) have a similar form.

2.2 Experimental Data and Parameters of the Model

The reference model consists of 12 differential equations. Eq. (1) is for the membrane potential V; Eq. (6) represents the general equation form for all 11 gating variables.

$$\frac{dV}{dt} = \frac{1}{C_m}\left(I_{\mathrm{Na}} + I_{\mathrm{K}} + I_{\mathrm{h}} + I_{\mathrm{Ca}} + I_{\mathrm{Leak}} + \frac{I_{\mathrm{inj}}}{I_{\mathrm{SA}}}\right) \tag{1}$$

$$I_{\mathrm{Na}} = (g_{\mathrm{Na_T}} m^3 h + g_{\mathrm{Na_P}} n)(E_{\mathrm{Na}} - V) \tag{2}$$

$$I_{\mathrm{K}} = (g_{\mathrm{K_{A1}}} b^4 + g_{\mathrm{K_{A2}}} p^4 q + g_{\mathrm{K_3}} u)(E_{\mathrm{K}} - V) \tag{3}$$

$$I_{\mathrm{h}} = g_{\mathrm{h}} z(-43 - V) \tag{4}$$

$$I_{\mathrm{K}} = (g_{\mathrm{Ca_H}} r^2 + g_{\mathrm{Ca_L}} s^2 t)(E_{\mathrm{Ca}} - V) \tag{5}$$

$$\frac{dx_j}{dt} = \frac{x_{j\infty}(V) - x_j}{\tau_j(V)} \qquad x = \{m, h, n, b, p, q, u, z, r, s, t\} \tag{6}$$

$$x_{\infty,j} = \frac{1}{2}\left[1 + \tanh\left(\frac{V - V_{1/2,j}}{\kappa_j}\right)\right] \tag{7}$$

$$\tau_j(V) = \tau_{0,j} + \tau_{\max,j}\left[1 - \tanh^2\left(\frac{V - V_{1/2,j}}{\sigma_j}\right)\right] \tag{8}$$

The experimental data was obtained by measuring membrane voltage of neurons in slices from adult male zebra finches. Neurons are assumed to be isolated without interacting with other neurons. Parameters in the model are determined by synchronizing experimental data with the mathematical model above.

The optimization was accomplished using the open source software IPOPT [7] on standard desktop hardware. The data assimilation window over which the model properties are estimated was 1500 ms long; the data were sampled at 50 kHz, resulting in 75,000 time points of voltage data. Common to direct method variational approaches, the model trajectories were co-located during the optimization procedure; that is, each component of $\{y_1(t), y_2(t), ..., y_{12}(t)\}$ was treated as an independent variable with the model dynamical equations imposed as equality constraints between neighboring time-points. Gating particle variables were constrained between 0 and 1, and each of the parameter was constrained between biologically realistic bounds. The 73 parameters of the model are presented in Appendix A.

The success of synchronization is validated by prediction behavior of model. The full model, with estimated parameters and state variables at t = 1500 ms, was then integrated forward for the remainder of the data epoch with the same injected current that was presented to the real neuron. One set of experimental data is synchronized as long as the prediction is identical with the recordings in experiments. (Fig. 1)

3 Reduction of Complex Model

An ideal reduction scheme is the one which produces the same dynamics as the reference model for equivalent parameter values. Insofar as our reduction preserves the

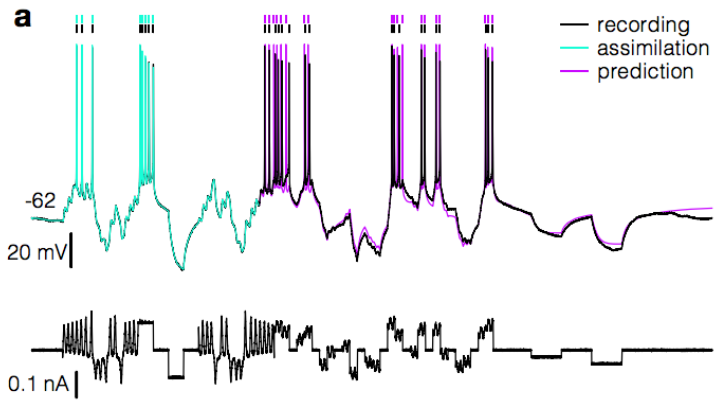

Figure 1: Data assimilation of HVc neuron model with experimental data: first 1500 ms data is used to estimate all the unobserved variables and unknown parameters, black line is experimental recording and cyan line is the result of synchronization. The last time step variable values are used as initial condition and fix parameters with estimated results, integrate full model and get the prediction (magenta line).

set of ionic currents in the reference model, we would like these currents to be similar in the two models. In terms of the function of the neuron within a network, only the temporal behavior of $V(t)$ is important because this is the only variable which is responsible for interactions among neurons. Hence, from this point of view, an ideal reduced model should have the same solutions, $V(t)$, as the solution of the original one for same parameter values. In relating the two models, there should be no change in the membrane potential $V(t)$. Unfortunately, it is usually impossible to find such a reduced model, and we formulate weaker requirements for a good reduction scheme.

It is assumed that all the parameters are fixed throughout the whole procedure of reduction. Hence, the effects of changing the parameters of the reference model is not tested in this project. This assumption is reasonable since all parameters of a single neuron within a functional network must be estimated from experimental data.

Kepler et al. [3] proposed a systematic strategy, the method of equivalent potentials, for the reduction of reference model. Since the equilibrium values of activation or inactivation variables are sigmoid functions of the membrane potential, these variables can be converted to equivalent potentials U_j defined by the equation

$$x_j = x_{j\infty}(U_j) \quad i.e. \quad U_j = x_{j\infty}^{-1}(x_j)$$

Here $x_{j\infty}^{-1}$ denotes the inverse function of $x_{j\infty}$. If several equivalent potentials U_j behave in a similar way under different conditions, a good approximation is to combine them together and represent them as one variable. A necessary condition for this grouping of variables is that their dynamics have similar time scales, i.e. the time constant are close. This method of combining several equivalent potentials into one is not unique. **?**] chose U by mimicking the time dependence of membrane potential equation in reference model. Kepler et al. [3] make a new representative equivalent potential taken

as a weighted average over all members of the group. Those weight coefficients are optimized to ensure the right value of the equilibrium potential at all values of external current and very nearly the correct stability and bifurcation characteristics. In the following procedure, we only choose one member of each group to represent all of them in order to test the effectiveness this method.

The equivalent potentials for activation and inactivation variables, compared with the membrane potential are presented in Fig. 2. The injected current is the same with Fig. 7. Equivalent potentials are considered as similar if their minimal and maximal values and their rise and fall times are close. Similarity can be seen between U_m and U_n, since gating variables m and n are the fastest two among 11 variables, with time constant $\tau = 0.01 \sim 0.03$ ms. U_h, U_u that respond more slowly than U_m, U_n, are responsible for the post-discharge refractoriness. They have time constant $\tau = 0.2 \sim 1$ ms. U_b, U_p, U_q, U_s have small amplitude oscillation with time constant of order 10^1 ms. U_r, U_t, U_z do not exhibit large amplitude oscillation since their time constants are of the order $10^2 \sim 10^3$ ms. Therefore, 11 variables are regrouped into four categories as plotted in Fig. 2.

We have grouped the variables according to the similarities of their dynamics:

1. The sodium activation variables $m,\ n$ in transient and persistent sodium currents, whose time scales are much faster than all the other activation and inactivation variables, which are considered as instantaneous: $m(t) = m_\infty(V(t))$ and $n(t) = n_\infty(V(t))$

2. Sodium inactivation h and slow potassium activation u response much lower than m, n, but much faster than other variables. The remarkable characteristic is that their equivalent potentials miss all the peaks of spikes. Here we keep U_h since sodium current is the most important current component. And the slow potassium activation u is taken as a function of U_h, the equivalent potential of the sodium inactivation variable: $u = u_\infty(U_h)$.

3. Gating variables b, p, q, s seem like have similar shapes that they increase when neuron is spiking and decrease when neuron is hyperpolarized. The trajectory of U_q looks different than those of the other three, as it doesn't go to the bottom of membrane potential at around 500 ms, since its half maximal voltage is different from the other three's. They are reduced to s by $b = b_\infty(U_s)$, $p = p_\infty(U_s)$, $q = q_\infty(U_s)$ This reduction is justified that the small change in gating variable doesn't make much difference in their corresponding currents.

4. The equivalent potential of r, t, z is much slower than all the other variables. Thus, they were held constant and regarded as a parameter. The average values over time are chosen for each of them: $r = r_\infty(\bar{U_r})$, $t = t_\infty(\bar{U_t})$, $z = z_\infty(\bar{U_z})$

Simply put, the dynamics of the combined variable is governed by the equation of motion of the most important variable in the group, i.e. the variable which contributes the most to changes in $V(t)$. This can be determined by comparing maximum conductance. After the above reduction, the remaining variables are h, s.

Therefore the reduced model has three variables (V, h, s) instead of the original 12. The equations defining the reduced model are the following:

$$\frac{dV}{dt} = \frac{1}{C_m}\left(I_{\mathrm{Na}} + I_{\mathrm{K}} + I_{\mathrm{h}} + I_{\mathrm{Ca}} + I_{\mathrm{Leak}} + \frac{I_{\mathrm{inj}}}{I_{\mathrm{SA}}}\right) \tag{9}$$

$$I_{\mathrm{Na}} = [g_{\mathrm{Na_T}} m_\infty^3(V)h + g_{\mathrm{Na_P}} n_\infty(V)](E_{\mathrm{Na}} - V) \tag{10}$$

$$I_{\mathrm{K}} = [g_{\mathrm{K_{A1}}} b_\infty^4(U_s) + g_{\mathrm{K_{A2}}} p_\infty^4(U_s) q_\infty(U_s) + g_{\mathrm{K_3}} u_\infty(U_h)](E_{\mathrm{K}} - V) \tag{11}$$

$$I_{\mathrm{h}} = g_{\mathrm{h}} z_\infty(\bar{U_z})(-43 - V) \tag{12}$$

$$I_{\mathrm{K}} = [g_{\mathrm{Ca_H}} r_\infty^2(\bar{U_r}) + g_{\mathrm{Ca_L}} s^2 t_\infty(\bar{U_t})](E_{\mathrm{Ca}} - V) \tag{13}$$

$$\frac{dx_j}{dt} = \frac{x_{j\infty}(V) - x_j}{\tau_j(V)} \quad x = \{h, s\} \tag{14}$$

$$x_{\infty,j} = \frac{1}{2}\left[1 + \tanh\left(\frac{V - V_{1/2,j}}{\kappa_j}\right)\right] \tag{15}$$

$$\tau_j(V) = \tau_{0,j} + \tau_{\max,j}\left[1 - \tanh^2\left(\frac{V - V_{1/2,j}}{\sigma_j}\right)\right] \tag{16}$$

4 Principal Component Analysis

We also looked at reducing the dimensionality of our model using principal component analysis (PCA). PCA is traditionally used to isolate the main degrees of variance in a dataset so we hoped it could reveal something about the nature of our model. We formulated our PCA problem by taking $V(t)$ and each $U_x(t)$ as dimensions in a 12 dimensional space. Thus each moment in time represents a point in this 12 dimensional space. So, taking all the data points in the time series from our reference model fit to an epoch of experimental data, to try and capture the number of degrees of freedom in the model. Performing PCA on the data yields the projection matrix, P from the equivalent potential space into the principal component space as well as the amount of variance each principal component is responsible for. The full list of variances are available in table 1, but the first two principal components represent 61.9% and 22.3% of variance whereas the last principal component explained only $7.4 \cdot 10^{-5}\%$ of the variance. To see how well our principal components describe our data we can then project the time series into principal component space using P, discard one of the dimensions by setting it to 0 and projecting back into potential space using P^{-1}. This is demonstrated in Fig. 3 and as we expect, even using only a couple principal components the reconstructed potential looks quite similar to the actual potential. We also notice that the differences are most noticeable at the peak of the action potential. This is due to the fact that in our data set, not much time is spent at the peak of an action potential so PCA doesn't have many examples of for it to include in its summary. It may be that the action potential peaks are undersampled using PCA.

This only indicates that the model spends most of its time approximately near the lower dimensional space defined by the first few principal components. This doesn't say that the model doesn't need all the degrees of freedom it uses to accurately predict

the behavior of the neuron. To do this, we try to integrate the differential equation while constraining it to the reduced dimensions. Since the differential equations are defined in the space of the gating variables and membrane potential, we choose to integrate in this space. In order to constrain it to the reduced principal component space we add a binding term to the calculated derivatives. Each time we calculate the derivative, dx, we calculate the equivalent potential, $y = f(x)$, of the given membrane gating values, x. Then we project y into the principal component space by $z = Py$ and filter out the less important principal components, by setting their values to 0 to get $\bar{z}$. Then we go back to the equivalent potential space by $\bar{y} = P^{-1}\bar{z}$. We calculate the derivative by converting $\bar{y}$ to $\bar{x} = f^{-1}(\bar{y})$ and calculating $d\bar{x}$ using our original differential equations. Then by differentiating $f^{-1}(y)$ and applying it to the difference between y and $\bar{y}$, we bind the solution to the reduced dimension space. The calculated derivative we use for our ordinary differential equation solver is $dx = d\bar{x} + f^{-1\prime}(\eta(y - \bar{y}))$. Where η is a binding parameter that determines how strongly the path is constrained to the reduced principal component space. Using a η about equal to 1 over the timestep of .0001 ms seemed to work somewhat, however the model is not particularly sensitive to η.

As expected when we run the algorithm with a complete reconstruction, it perfectly reconstructs integration provided by the reference model. However, when we remove a single principal component, which accounts for only $7.4 \cdot 10^{-5}\%$ of the variance, the integrated path differs quite a bit from our reference model as can be seen in Fig 4. Here it can be noted that the reduced model is much more sensitive to initial conditions because whereas our reference model quickly returns to its resting state, the atypical initial values used don't lie in the reduced principal component space making it more difficult to reach the resting state. The spiking behavior also differs slightly for the aforementioned reasons. Interestingly, at around 450 ms the limited model fits the recorded membrane potential better than our reference model. While the reference model generates a series of minispikes, the reduced model behaves more similarly to the rough resting state of the actual neuron. Overall, however, it was surprising that removal of a single principle component resulted in so much of a difference in the behavior of the model. In fact, removal of a second principal component, caused the integration to fail and we were unable to complete the integration as shown in Fig 5.

This result was quite surprising because the eleventh principal component explained only $2.1 \cdot 10^{-3}\%$ of the variance in the data. However, when you compare this value to the $7.4 \cdot 10^{-5}\%$ explained by the twelfth principal component which resulted in significant differences, It makes a bit more sense.

5 Discussion

To assess the quality of the reduced model, we compared it with the reference model using the same initial condition and same parameters. Firstly, we compared the same data set that we used for reduction to see whether reduced model can repeat the behavior. We can see from Fig. 6. The trajectory of voltage in reduced model doesn't overlap that of reference model. Especially at the peak of spikes, reduced model are much higher than reference model. As we retrieved back to reference from reduced

Table 1: Percent of variance explained by each principal component. For example, removing only the 12th principal component should only remove $7.4 \cdot 10^{-5}$ % of the variance of our data.

Principal Component	Variance Explained (%)
1	62.9
2	22.3
3	11.0
4	2.6
5	1.2
6	0.45
7	0.28
8	0.22
9	$4.8 \cdot 10^{-2}$
10	$4.1 \cdot 10^{-2}$
11	$2.1 \cdot 10^{-3}$
12	$7.4 \cdot 10^{-5}$

model, we find this big error comes from the reduction of gating variables h and u. As we can see from Fig. 2.b, the maximals decrease in order V, U_u, U_h. If we simply replace U_u with U_h, it will make great difference in membrane voltage V. Here we used principal component analysis to find a linear combination of U_h and V to represent U_u. The result we got using the PCA analysis tool in python matplotlib library is that U_u can be expressed as $U_u = 0.5V + 0.5U_h$. After that, the behavior of reduced model has been improved a lot. (Fig. 7) It also tells us this method might fail in some special case.

An ideal reduced model should have the same temporal behavior of $V(t)$, as that of the original one for same parameter values and initial conditions under arbitrary injected current. Reduced model is also tested with arbitrary injected current, the results are in excellent agreement with experimental data. (Fig. 8)

6 Summary

We have produced a simplification of this model that has three-dimensional phase by using the method of equivalent potentials, suggested by Kepler et al to combine several dynamical variables with similar time scales. Phase-dimensionality of reference model is successfully reduced from 12 to 3. Membrane potentials have identical behavior in reference and reduced model, and it holds for arbitrary injected current under certain parameters. Although PCA initially seemed a promising lead towards understanding the reduction of our model, it turns out PCA had trouble dealing with the non-linearities in our differential equations, limiting its usefulness.

References

[1] A. L. Hodgkin and A. F. Huxley. A quantitative description of membrane current and its application to conduction and excitation in nerve. *The Journal of Physiology*, 117(4):500–544, 1952.

[2] V. I. Krinskii and Yu. M. Kokoz. Analysis of the equations of excitable membranes. i. reduction of the hodgkins-huxley equations to a 2d order system. *Biofizika*, 18: 506511, 1973.

[3] Thomas B. Kepler, L.F. Abbott, and Eve Marder. Reduction of conductance-based neuron models. *Biological Cybernetics*, 66:381–387, 1992. ISSN 0340-1200. doi: 10.1007/BF00197717.

[4] David Golomb, John Guckenheimer, and Shay Gueron. Reduction of a channel-based model for a stomatogastric ganglion lp neuron. *Biological Cybernetics*, 69: 129–137, 1993. ISSN 0340-1200. doi: 10.1007/BF00226196. URL `http://dx.doi.org/10.1007/BF00226196`.

[5] Yoshinobu Maeda, K. Pakdaman, Taishin Nomura, Shinji Doi, and Shunsuke Sato. Reduction of a model for an onchidium pacemaker neuron. *Biological Cybernetics*, 78(4):265, 1998. ISSN 03401200. URL `http://search.ebscohost.com/login.aspx?direct=true&db=eih&AN=4678122&site=ehost-live`.

[6] Daniel C. Meliza, Mark Kostuk, Hao Huang, Alain Nogaret, Henry D. I. Abarbanel, and Daniel Margoliash. Dynamical state and parameter estimation validated by prediction of experimental membrane voltages for conductance-based models of individual neurons. *private communication*, 2012.

[7] Andreas Wchter and Lorenz T. Biegler. On the implementation of an interior-point filter line-search algorithm for large-scale nonlinear programming. *Mathematical Programming*, 106:25–57, 2006. ISSN 0025-5610. doi: 10.1007/s10107-004-0559-y. URL `http://dx.doi.org/10.1007/s10107-004-0559-y`.

A Complete Model and Parameters Values

The complete set of model equations that are used for the optimization procedure, including the synchronization-inspired regularization term are given here.

$$
\begin{aligned}
dy_1/dt =&((p_2 y_2^3 y_3 + p_3 y_4)(p_4 - y_1) + (p_5 y_5^4 + p_6 y_6^4 y_7 + p_7 y_8)(p_8 - y_1) \\
&+ (p_{71} y_9^2 + p_{72} y_{10}^2 y_{11}) 19.2970673 (p_{11} - 0.0001 \exp(y_1/13))/\text{GHK} \\
&+ p_9(p_{10} - y_1) + p_{12} y_{12}(-43 - y_1) + I_{inj}/p_{13})/p_1 + \gamma(V_{data} - y_1) \\
dy_2/dt =&0.5(1 + \tanh((y_1 - p_{14})/p_{15}) - 2y_2)/(p_{17} + p_{18}(1 - \tanh^2((y_1 - p_{14})/p_{16}))) \\
dy_3/dt =&0.5(1 + \tanh((y_1 - p_{19})/p_{20}) - 2y_3)/(p_{22} + p_{23}(1 - \tanh^2((y_1 - p_{19})/p_{21}))) \\
dy_4/dt =&0.5(1 + \tanh((y_1 - p_{24})/p_{25}) - 2y_4)/(p_{27} + p_{28}(1 - \tanh^2((y_1 - p_{24})/p_{26}))) \\
dy_5/dt =&0.5(1 + \tanh((y_1 - p_{29})/p_{30}) - 2y_5)/(p_{32} + p_{33}(1 - \tanh^2((y_1 - p_{29})/p_{31}))) \\
dy_6/dt =&0.5(1 + \tanh((y_1 - p_{34})/p_{35}) - 2y_6)/(p_{37} + p_{38}(1 - \tanh^2((y_1 - p_{34})/p_{36}))) \\
dy_7/dt =&0.5(1 + \tanh((y_1 - p_{39})/p_{40}) - 2y_7)/(p_{42} + p_{44} + 0.5(1 - \tanh(y_1 - p_{39})) \\
&\cdot (p_{43}(1 - \tanh^2((y_1 - p_{39})/p_{41})) - p_{44})) \\
dy_8/dt =&0.5(1 + \tanh((y_1 - p_{45})/p_{46}) - 2y_8)/(p_{48} + p_{49}(1 - \tanh^2((y_1 - p_{45})/p_{47}))) \\
dy_9/dt =&0.5(1 + \tanh((y_1 - p_{50})/p_{51}) - 2y_9)/(p_{53} + p_{54}(1 - \tanh^2((y_1 - p_{50})/p_{52}))) \\
dy_{10}/dt =&0.5(1 + \tanh((y_1 - p_{55})/p_{56}) - 2y_{10})/(p_{58} + p_{59}(1 - \tanh^2((y_1 - p_{55})/p_{57}))) \\
dy_{11}/dt =&0.5(1 + \tanh((y_1 - p_{60})/p_{61}) - 2y_{11})/(p_{64} + p_{65}(1 + \tanh((y_1 - p_{60})/p_{62})) \\
&\cdot (1 - \tanh((y_1 - p_{60})/p_{63}))(1 - \tanh(y_1 - p_{60}) \tanh((1/p_{62} + 1/p_{63})(y_1 - p_{60}))) \\
&/(1 + \tanh((y_1 - p_{60})/p_{62}) \tanh((y_1 - p_{60})/p_{63}))) \\
dy_{12}/dt =&0.5(1 + \tanh((y_1 - p_{66})/p_{67}) - 2y_{12})/(p_{69} + p_{70}(1 - \tanh^2((y_1 - p_{66})/p_{68})))
\end{aligned}
\tag{17}
$$

Where the GHK expansion is given by:

$$
\begin{aligned}
\text{GHK} =&(1 + y_1/26(1 + y_1/39(1 + y_1/52(1 + y_1/65(1 + y_1/78(1 + y_1/91(1 + y_1/104 \\
&(1 + y_1/117(1 + y_1/130(1 + y_1/143(1 + y_1/156(1 + y_1/169(1 + y_1/182(1 + y_1/195 \\
&(1 + y_1/208(1 + y_1/221(1 + y_1/234(1 + y_1/247(1 + y_1/260(1 + y_1/273(1 + y_1/286 \\
&(1 + y_1/299(1 + y_1/312(1 + y_1/325))))))))))))))))))))))))))
\end{aligned}
$$

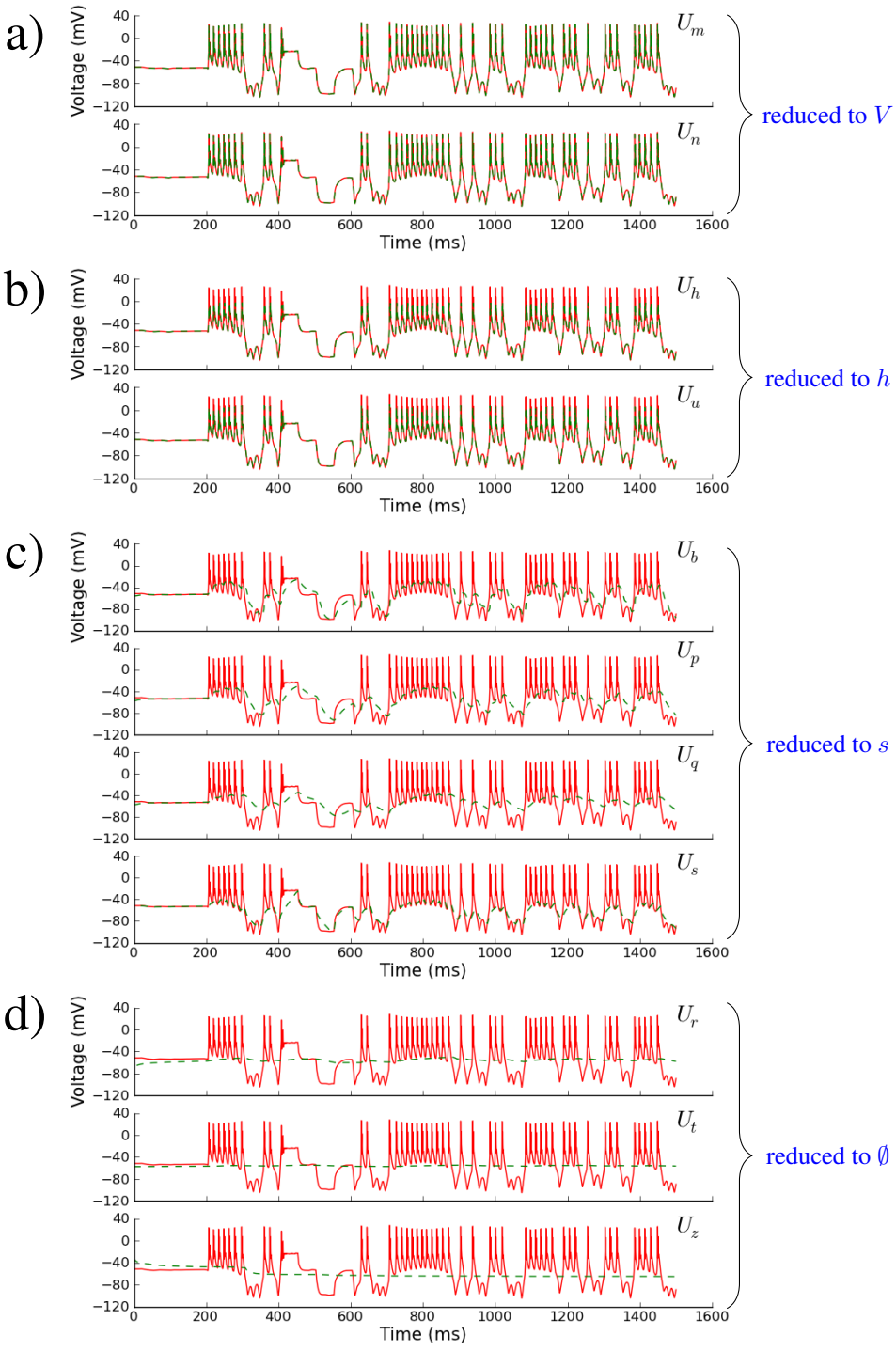

Figure 2: Equivalent potentials (green dash line) of 11 gating variables compared with membrane potential (red solid line). They are classified into four categorizes according to their constant rate τ^{-1}.

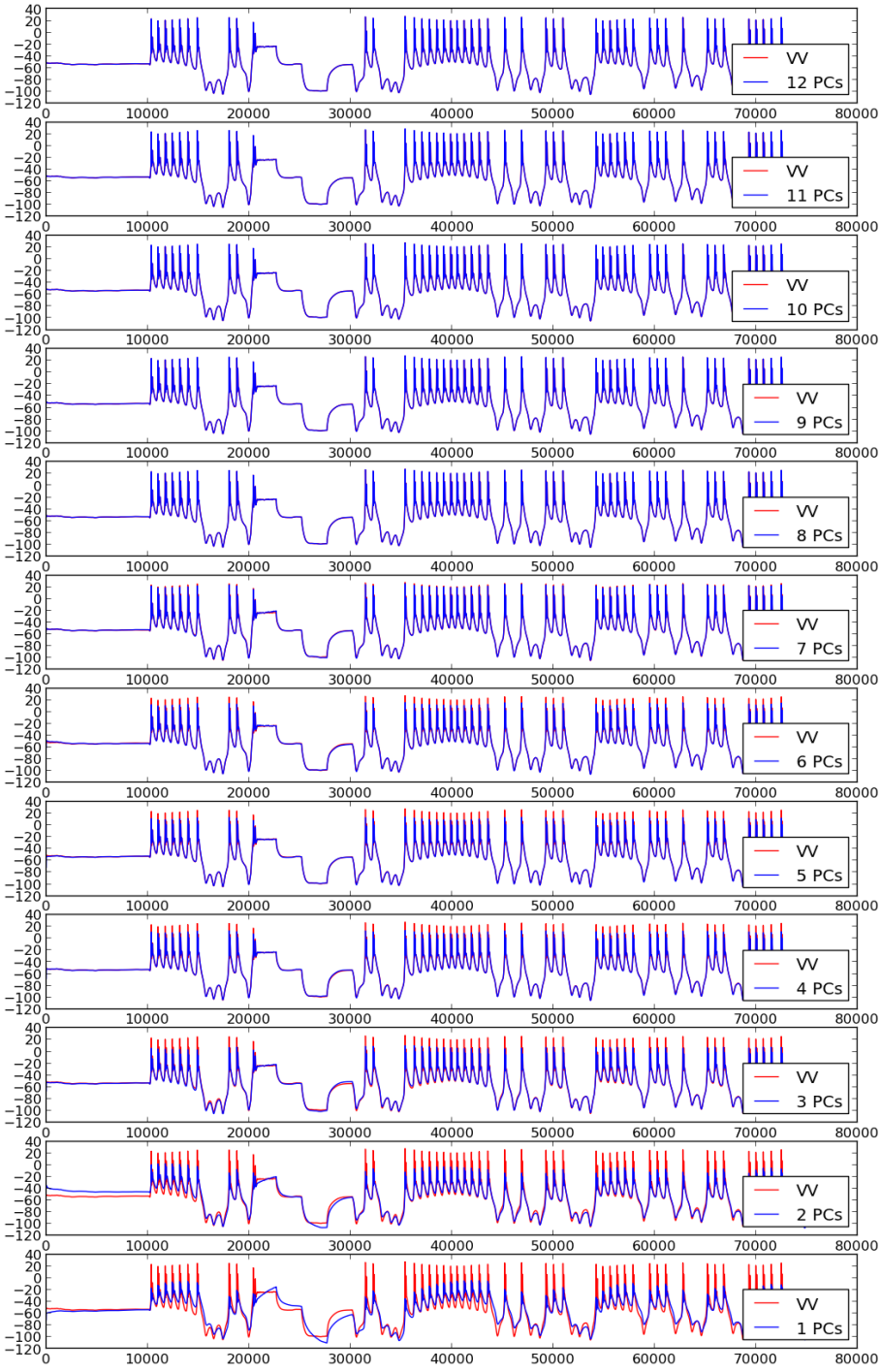

Figure 3: Reconstruction of the membrane potential using varied amounts of principal components (blue) compared to the membrane potential of the reference model. As expected, using all the principal components completely reconstructs the reference model's estimate, and as you reduce the principal components it reduces the similarity to the reference model's membrane potential, however, even using just a single principal component, the membrane potential is still somewhat recognizable.

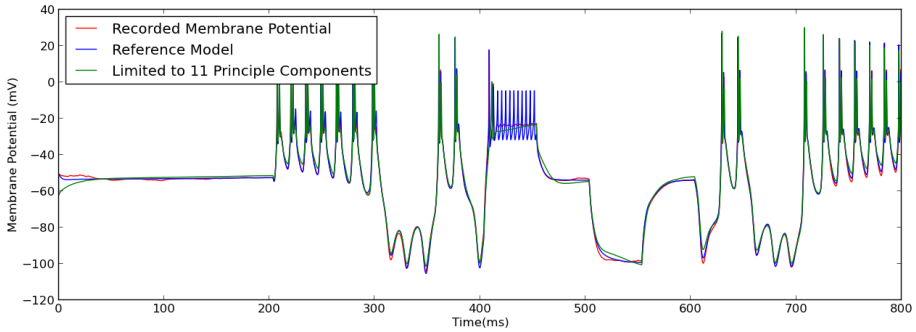

Figure 4: Reference model constrained to 11 of 12 principal components. Constraint method described in detail in section 4.

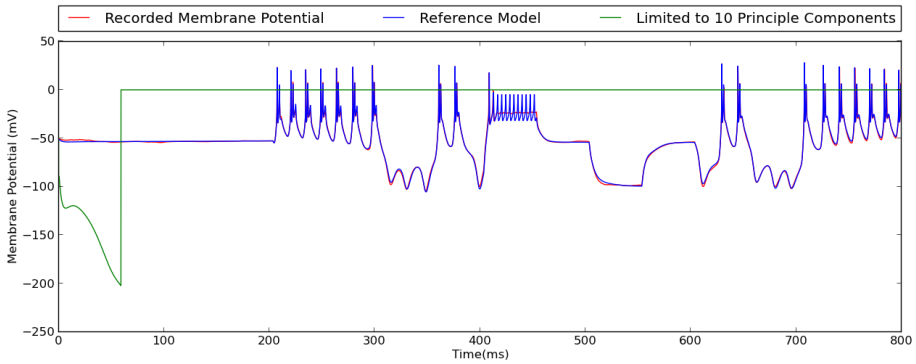

Figure 5: Reference model constrained to 10 of 12 principal components. Constraint method described in detail in section 4. The ordinary differential equation solver was unable to integrate this differential equation, perhaps because of the stiffness of the problem.

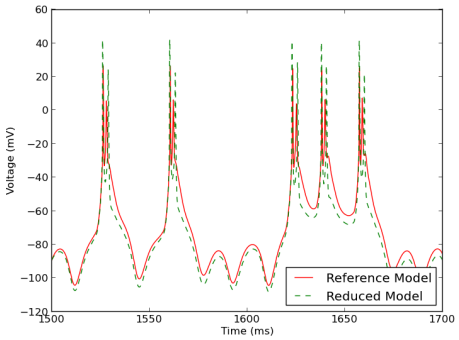

Figure 6: Preliminary result of reduced model: We combine all equivalent potential variables simply by replacing all of them by one of them. Note that the peak potential achieved by action potentials is lower in the reduced model than that of reference model.

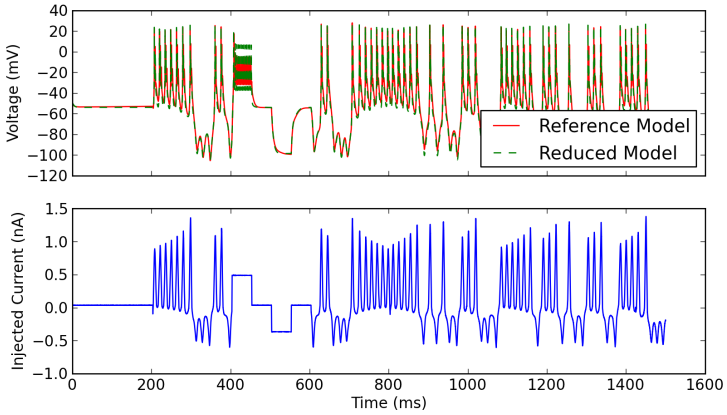

Figure 7: Comparison of reference model and reduced model: data is obtained by integrating the two models using the same initial condition and same parameters.

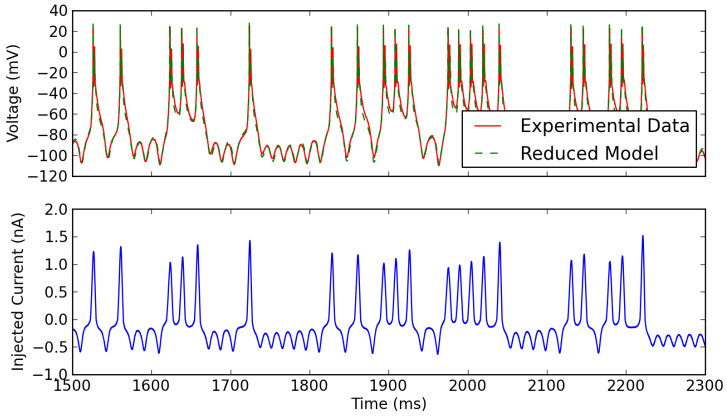

Figure 8: Comparison of reduced model data and experimental data: initial condition is found using the first 100 ms data and the rest of the data is integrated using the reduced model

Table 2: The complete list of optimization bounds and model parameter estimates.

param number	param 'name'	lower bound	upper bound	neuron N1	neuron N2	neuron N3
p_1	Cm	0.900	1.100	1.100	1.032	1.035
p_2	gNaT	5.000	170.000	7.545	85.364	9.736
p_3	gNaP	0.000	20.000	0.008	0.086	0.075
p_4	ENa	45.000	55.000	55.000	55.000	55.000
p_5	gKA1	0.000	80.000	0.096	0.216	0.000
p_6	gKA2	0.000	80.000	5.687	14.708	1.074
p_7	gKc	0.000	12.000	0.438	0.191	6.482
p_8	EK	-85.000	-70.000	-75.001	-85.000	-85.000
p_9	gL	0.010	0.600	0.010	0.036	0.047
p_{10}	EL	-65.000	-48.000	-65.000	-65.000	-65.000
p_{11}	CaExt	0.010	9.000	0.020	9.000	8.996
p_{12}	gH	0.000	10.000	0.017	0.011	0.000
p_{13}	Isa	0.015	0.250	0.038	0.081	0.078
p_{14}	amV1	-45.000	-15.000	-34.738	-18.495	-38.400
p_{15}	amV2	0.500	25.000	21.682	22.457	17.327
p_{16}	amV3	0.500	25.000	0.500	0.500	0.500
p_{17}	tm0	0.010	0.700	0.010	0.194	0.010
p_{18}	epsm	0.012	7.000	0.012	0.158	0.012
p_{19}	ahV1	-75.000	-35.000	-43.132	-38.452	-57.314
p_{20}	ahV2	-25.000	-0.500	-9.400	-4.487	-25.000
p_{21}	ahV3	5.000	25.000	6.401	22.344	5.000
p_{22}	th0	0.020	2.000	0.554	0.207	0.841
p_{23}	epsh	1.000	30.000	30.000	4.427	21.173
p_{24}	anV1	-69.000	-29.000	-64.537	-37.719	-57.822
p_{25}	anV2	5.000	25.000	5.000	5.349	11.042
p_{26}	anV3	5.000	25.000	25.000	5.194	25.000
p_{27}	tn0	0.020	2.000	2.000	0.020	1.088
p_{28}	epsn	0.012	7.000	7.000	7.000	0.012
p_{29}	abV1	-69.000	-21.000	-67.970	-54.343	-67.597
p_{30}	abV2	5.000	25.000	6.734	15.528	24.998
p_{31}	abV3	5.000	25.000	7.908	5.000	24.992
p_{32}	tb0	0.020	2.000	2.000	0.052	1.998
p_{33}	epsb	1.000	30.000	30.000	1.000	29.979
p_{34}	apV1	-90.000	-21.000	-52.893	-41.932	-66.958
p_{35}	apV2	5.000	48.000	13.597	10.972	19.837
p_{36}	apV3	5.000	48.000	11.528	48.000	45.659
p_{37}	tp0	0.020	2.000	0.020	0.020	2.000
p_{38}	epsp	1.000	30.000	1.838	1.000	30.000

Table 3: (cont.) The complete list of optimization bounds and model parameter estimates.

param number	param 'name'	lower bound	upper bound	neuron N1	neuron N2	neuron N3
p_{39}	aqV1	-90.000	-35.000	-66.425	-52.586	-73.699
p_{40}	aqV2	-39.000	-5.000	-30.417	-11.517	-24.863
p_{41}	aqV3	-39.000	-5.000	-39.000	-20.389	-5.000
p_{42}	tq0	0.020	2.000	2.000	1.989	0.020
p_{43}	epsq	0.500	100.000	68.490	100.000	0.663
p_{44}	deltasq	0.000	30.000	2.113	0.000	22.460
p_{45}	auV1	-15.000	40.000	-15.000	-15.000	5.976
p_{46}	auV2	5.000	65.000	65.000	65.000	37.251
p_{47}	auV3	5.000	70.000	70.000	20.202	6.190
p_{48}	tu0	0.020	55.000	55.000	0.020	1.106
p_{49}	epsu	1.000	150.000	150.000	128.333	2.561
p_{50}	arV1	-56.000	-8.000	-55.999	-49.049	-55.998
p_{51}	arV2	5.000	49.000	48.995	29.827	48.991
p_{52}	arV3	5.000	55.000	54.990	54.855	54.909
p_{53}	tr0	0.020	2.000	1.966	0.020	1.863
p_{54}	epsr	1.000	295.000	294.917	6.273	294.835
p_{55}	asV1	-80.000	-35.000	-71.954	-44.457	-71.213
p_{56}	asV2	5.000	39.000	38.987	30.094	20.336
p_{57}	asV3	5.000	57.000	56.983	22.726	57.000
p_{58}	ts0	0.020	2.000	1.975	0.020	2.000
p_{59}	eps5	1.000	150.000	149.945	110.617	19.396
p_{60}	atV1	-90.000	-55.000	-72.996	-56.002	-55.000
p_{61}	atV2	-34.000	-5.000	-33.759	-7.789	-34.000
p_{62}	atV3	3.000	55.000	54.853	55.000	55.000
p_{63}	atV4	3.000	55.000	54.824	4.362	55.000
p_{64}	tx0	5.000	190.000	189.147	59.808	190.000
p_{65}	epst	0.500	7000.000	6959.019	7000.000	7000.000
p_{66}	azV1	-90.000	-40.000	-89.061	-63.231	-67.150
p_{67}	azV2	-40.000	-5.000	-6.416	-5.000	-38.150
p_{68}	azV3	5.000	40.000	13.075	40.000	38.297
p_{69}	tz0	0.020	2.000	2.000	2.000	1.029
p_{70}	epsz	100.000	2000.000	2000.000	2000.000	1925.350
p_{71}	gCaL	0.000	10.000	0.000	0.010	0.000
p_{72}	gCaT	0.000	10.000	0.000	0.003	0.004